

NON-NEWTONIAN MHD MIXED CONVECTIVE POWER-LAW FLUID FLOW OVER A VERTICAL STRETCHING SHEET WITH THERMAL RADIATION, HEAT GENERATION AND CHEMICAL REACTION EFFECTS

Md. Shakhaoath Khan, Ifsana Karim, Md. Haider Ali Biswas
Mathematics Discipline; Science, Engineering and Technology School,
Khulna University, BANGLADESH.

shakhaoathmathku@yahoo.com, simimathku@gmail.com, mhabiswas@yahoo.com

ABSTRACT

In the present approach, the problem of MHD mixed convective flow and heat and mass transfer of an electrically conducting non-Newtonian power-law fluid past a vertical stretching surface in the presence of thermal radiation, heat generation and chemical reaction is considered. The stretching velocity, temperature and concentration are assumed to vary in a power-law with the distance from the origin. The flow is induced due to an infinite elastic sheet which is stretched in its own plane. The governing equations are reduced to non-linear ordinary coupled differential equations by means of similarity transformations. These equations are then solved numerically by the Nactsheim-Swigert shooting technique together with Runge-Kutta six order iteration schemes. The numerical solution is found to be dependent on several governing parameters, including the magnetic parameter, power-law index, thermal conductive parameter/mixed convection parameter, mass convective parameter, radiation parameter, modified Prandtl number, heat source parameter, chemical reaction parameter and Schmidt number. A systematic study is carried out to illustrate the effects of these parameters on the fluid velocity and the temperature and distribution in the boundary layer. The results for the local skin-friction coefficient and the local Nusselt number are tabulated and discussed. Comparison with previously published work is performed and excellent agreement is observed. The results obtained several many interesting behaviors that warrant further study on the equations related to non-Newtonian fluid phenomena.

Keywords: Power-Law Fluid; Vertical stretching sheet; Thermal Radiation; Heat Generation; Chemical Reaction.

INTRODUCTION

The study of Magnetohydrodynamics (MHD) boundary layer flows have stimulated extensive attention due to its significant applications in three different subject areas, such as astrophysical, geophysical and engineering problems. Radiation effects on convection can be quite important in the context of many industrial applications involving high temperatures such as nuclear power plant, gas turbines and various propulsions engines for aircraft technology. In many chemical engineering processes, chemical reactions take place between a foreign mass and the working fluid which moves due to the stretch of a surface. The order of chemical reaction depends on several factors. One of the simplest chemical reactions is the first order reaction in which the rate of the reaction is directly proportional to the species concentration. Chemical reaction can be classified as either homogeneous or heterogeneous processes, which depends on whether it occurs at an interface or as a single-phase volume reaction. In most cases of chemical reactions, the reaction rate depends on the concentration of the species itself. During the past four decades the study of non-Newtonian fluids has gained interest because of their numerous technological applications, including manufacturing of plastic sheets, performance of lubricants, and movement of biological fluids. Hence the study of non-Newtonian fluid flow is important, different models have been proposed to explain the behavior of non-Newtonian fluid. Among these, the power law, the differential type, and the rate type models gained importance. The knowledge of flow and heat mass transfer within a thin liquid film is crucial in understanding the coating process, designing of heat exchangers and chemical processing equipments. This interest stems from many engineering and geophysical applications such as geothermal reservoirs and other applications including wire and fiber coating, food stuff processing, reactor fluidization, transpiration cooling, thermal insulation, enhanced oil recovery, packed bed catalytic reactors, cooling of nuclear reactors and underground energy transport. The prime aim in

almost every extrusion is to maintain the surface quality of the extricate. All coating processes demand a smooth glossy surface to meet the requirements for the best appearance and optimum service properties such as low friction, transparency and strength. In particular, the flow of an incompressible non-Newtonian fluid over a stretching sheet has several industrial applications in, for example, extrusion of a polymer sheet from a dye or in the drawing of plastic films. In view of their differences with Newtonian fluids, several models of non-Newtonian fluids have been pro-posed. Amongst these the simplest and the most common model is the power-law fluid, which has received special attraction from the researchers in the field. Acrivos (1960) investigated the theoretical analysis of laminar natural convection heat transfer to non-Newtonian fluids. Schowalter (1960) was among pioneer researchers, who studied the application of boundary layer to power law pseudo-plastic fluids.

Since the pioneering work various aspects of the stretching sheet problem involving Newtonian/non-Newtonian fluids have been extensively studied by several authors. Some recent papers in this direction may be found in the references Crane (1970), Gupta & Gupta (1977), Jadhav & Waghmode (1990). These research works do not however consider the situation where hydro magnetic effects arise. The study of hydrodynamic flow and heat transfer over a stretching sheet may find its applications in polymer technology related to the stretching of plastic sheets. Also, many metallurgical processes involve the cooling of continuous strips or filaments by drawing them through a quiescent fluid and while drawing these strips are sometimes stretched. The rate of cooling can be controlled by drawing such strips in an electrically conducting fluid subjected to a magnetic field in order to get the final products of desired characteristics; as such a process greatly depends on the rate of cooling. In view of this, the study of MHD flow of Newtonian/non-Newtonian flow over a stretching sheet was carried out by many researchers Sarpakaya (1961), Pavlov (1974), Andersson *et al.*, (1992), Char (1994), Cortell (2005).

In recent decades several industrial processes deal with the power law fluid flows with magnetic field, Zhang & Wang (2007) discussed on the similarity solutions of Magnetohydrodynamics flows of power-law fluids over a stretching sheet. Thermal radiation effects often occur in particular at high temperature processes including glass manufacturing, combustion operation and nuclear power plant. Rosseland diffusion flux model, which is viable for the optically thick flows is utilized to analyze the problem, successfully some researchers Lio (2005), Khan *et al.*, (2011) put forward work on radiation effects of MHD flow and heat transfer of the electrically conducting fluid over a stretching sheet. Cheng & Minkowycz (1977) studied free convection from a vertical flat plate with applications to heat transfer from a disk. Gorla *et al.*, (1987-88) solved the non similar problem of free convective heat transfer from a vertical plate embedded in a saturated porous medium with an arbitrary varying surface temperature.

Very recent Prasad *et al.*, (2012) studied the problem of magneto-hydrodynamic flow and heat transfer of an electrically conducting non-Newtonian power-law fluid past a non-linearly stretching surface in the presence of a transverse magnetic field. Azeem & Ramzan (2012) investigated a rigorous mathematical analysis is given for a magneto-hydrodynamic flow and heat transfer of a power law fluid over a vertically stretching surface.

In view of these practical applications and analyses, the main concern of the present paper is to study the effect of thermal radiation, heat generation and chemical reaction on the MHD power-law fluid flow and heat and mass transfer over a vertical stretching sheet. This extends the work of Azeem & Ramzan (2012), to the case of MHD non-Newtonian power-law fluid flow heat and mass transfer by considering the contribution of heat generation and chemical reaction. Because of the intricacy, the influence of the magnetic parameter (M), power-law index (n), thermal conductive parameter/mixed convection parameter (λ), mass convective parameter (λ_m), radiation parameter (N_r), modified Prandtl number (P_r), heat source parameter (Q), chemical reaction parameter (γ) and Schmidt number (S_c) make the momentum, energy and concentration equations coupled and highly non-linear partial differential equations. To reduce the number of independent variables, these partial differential equations are simplified to couple non-linear ordinary differential equations by suitable similarity transformations. The obtained non linear coupled ordinary differential equations are solved

numerically using Nactsheim-Swigert (Nactsheim & Swigert (1965) shooting iteration technique together with Runge-Kutta six order iteration schemes. The velocity, temperature and concentration distributions are discussed and presented graphically, and also the skin-friction coefficient, the surface heat and mass transfer rate at the sheet are investigated.

MATHEMATICAL FORMULATION

Consider the steady state, incompressible, mixed convection boundary layer flow of an electrically conducting power-law fluid in the presence of the transverse magnetic field over a vertical stretching sheet. The induced magnetic field and polarizations are neglected. The positive x -axis is assumed along the direction of the flow and y -axis measured normal to the sheet. The radiation effects are taken into account. The flow phenomena generated as a result of linear stretching of sheet.

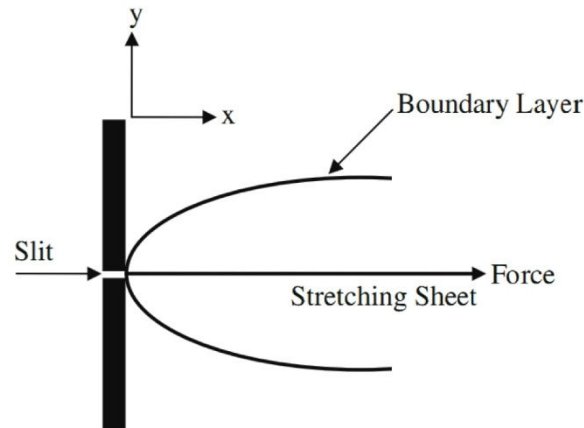


Figure 1. Physical Configuration and coordinates system.

Assumed the continuous linear stretching velocity of the form, $U(x)=ax$ where a is the linear stretching constant and x is the distance from origin. Under boundary layer approximations, the continuity, momentum, energy and concentration equations are given by

The Continuity Equation

$$\frac{\partial u}{\partial x} + \frac{\partial v}{\partial y} = 0 \quad (1)$$

The Momentum Equation

$$u \frac{\partial u}{\partial x} + v \frac{\partial u}{\partial y} = -\frac{k}{\rho} \frac{\partial}{\partial y} \left(-\frac{\partial u}{\partial y} \right)^n - \frac{\sigma B_0^2}{\rho} u \pm g\beta(T - T_\infty) \pm g\beta^*(C - C_\infty) \quad (2)$$

The Energy Equation

$$u \frac{\partial T}{\partial x} + v \frac{\partial T}{\partial y} = \alpha \frac{\partial^2 T}{\partial y^2} + \frac{Q_\infty}{\rho c_p} (T - T_\infty) - \left(\frac{1}{\rho c_p} \right) \frac{\partial q_r}{\partial y} \quad (3)$$

The Concentration Equation

$$u \frac{\partial C}{\partial x} + v \frac{\partial C}{\partial y} = D \frac{\partial^2 C}{\partial y^2} - K_r (C - C_\infty). \quad (4)$$

In the above u and v are velocity components along x and y axis respectively. n is the power law index, B_0 is the induced magnetic field, ρ is the density of the fluid, σ is the charge density, g is the acceleration due to gravity, β is the thermal expansion coefficient, β^* is the mass expansion coefficient, T is the temperature of the fluid, C is the concentration of the fluid, α is the thermal

diffusivity, k is the thermal conductivity of the fluid, q_r is the radiative heat flux, Q_c is the heat generation coefficient, D is the mass diffusion coefficient and K_r is the rate of chemical reaction. In equation (2) the first term in the right hand side is the shear rate and assumed as negative throughout the boundary layer, also the velocity component decreases with the distance y for continuous stretching surface. In the present context no pressure gradient is exerted, instead the flow is driven solely by a flat stretched surface, which moves with a velocity $U(x)$, the last two term in the right hand side represents the influence of thermal and mass buoyancy force on the flow field, where $+$ the buoyancy assisting and $-$ for buoyancy opposing the flow region respectively. The buoyancy assisting is represented in the positive x -axis, which is in vertically upward in the flow direction and buoyancy opposing is in the downward direction, in the case the stretching induced flow and the thermal buoyancy flow balance each other. The applicable boundary conditions for the model are;

$$u(x, y) = u(x) = U = ax, v(x, y) = 0, T = T_\infty + A_1 \left(\frac{x}{l} \right), C = C_\infty + A_2 \left(\frac{x}{l} \right) \text{ at } y = 0 \quad (5)$$

$$u(x, y) \rightarrow 0, T(x, y) \rightarrow T_\infty, C(x, y) \rightarrow C_\infty \text{ as } y \rightarrow \infty \quad (6)$$

where, $u(x)$ is the stretching velocity, a is the linear stretching constant, l is the characteristics length and A_1, A_2 is the constant whose values depends on the properties of the fluid.

Rosseland approximation (1992) has been considered for radiative heat flux and leads to the form as,

$$q_r = -\frac{4\sigma}{3\kappa^*} \frac{\partial T^4}{\partial y} \quad (7)$$

where σ is the Stefan-Boltzmann constant and κ^* is the mean absorption coefficient. The temperature difference with in the flow is sufficiently small such that T^4 may be expressed as a linear function of the temperature, then the Taylor's series for T^4 about T_∞ after neglecting higher order terms,

$$T^4 = 4T_\infty^3 - 3T_\infty^4 \quad (8)$$

In order to attains a similarity solution to equations (1) to (4) with the boundary conditions (5) and (6), the following dimensionless variables are used,

$$\eta = \frac{y}{x} (\text{Re}_x)^{\frac{1}{n+1}}, \psi(x, y) = Ux (\text{Re}_x)^{\frac{1}{n+1}} f(\eta), \theta = \theta(\eta) = \frac{T - T_\infty}{T_f - T_\infty}, \phi(\eta) = \frac{C - C_\infty}{C_f - C_\infty} \quad (9)$$

The velocity components in terms of stream function are defined as

$$u = \frac{\partial \psi}{\partial y}, v = -\frac{\partial \psi}{\partial x} \quad (10)$$

From the above transformations the non dimensional, nonlinear, coupled ordinary differential equations are obtained as;

$$n(-f'')^{n-1} f''' - f'^2 + \left(\frac{2n}{n+1} \right) ff'' - Mf' + \lambda\theta + \lambda_M\phi = 0 \quad (11)$$

$$\left(1 + \frac{4}{3} N_r \right) \theta'' + P_r \left(\frac{2n}{n+1} f\theta' - f'\theta + Q \cdot \theta \right) = 0 \quad (12)$$

$$\phi'' + \left(\frac{2n}{n+1} \right) S_c f\phi' - \gamma R_{ex} S_c \phi = 0 \quad (13)$$

and the corresponding boundary conditions,

$$\left. \begin{aligned} f = 0, f' = 1, \theta = 1, \varphi = 1, \text{ at } \eta = 0 \\ f' = 0, \theta = 0, \varphi = 0, \quad \text{as } \eta \rightarrow \infty \end{aligned} \right\} \quad (14)$$

Where the notation primes denote differentiation with respect to η and the parameters are defined as

$$M = \frac{2\sigma B_0^2}{\rho a} \quad (\text{Magnetic parameter})$$

$$N_r = \frac{4\sigma T_\infty^3}{3k\kappa^*} \quad (\text{Radiation parameter})$$

$$p_r = \frac{ax^2}{\alpha} (\text{Re}_x)^{\frac{2}{n+1}} \quad (\text{Modified Prandtl number})$$

$$\lambda = \pm \frac{Gr_x}{\text{Re}_x} \quad (\text{Thermal convective parameter})$$

$$\lambda_M = \pm \frac{Gm_x}{\text{Re}_x} \quad (\text{Mass convective parameter})$$

$$Gr_x = \frac{g\beta(T_f - T_\infty)\rho x a^{-n}}{k} \quad (\text{Local Grashof number})$$

$$Gm_x = \frac{g\beta^*(C_f - C_\infty)\rho x a^{-n}}{k} \quad (\text{Modified Grashof number})$$

$$Q = \frac{Q_0}{\rho C_p a} \quad (\text{Heat source parameter})$$

$$S_c = \frac{\nu}{D} \quad (\text{Schmidt number})$$

$$\gamma = \frac{\nu k_r}{U^2} \quad (\text{Chemical reaction parameter})$$

and $\text{Re}_x = \frac{\rho U^{2-n} x^n}{k} \quad (\text{local Reynolds number}).$

The physical quantities of the reduced Nusselt number and reduced Sherwood number are calculated respectively by the following equations,

$$C_f = \frac{\tau_w(x)}{\left(\frac{\rho u^2}{2}\right)} \quad \text{with } \tau_w(x) = \mu \left(\frac{\partial u}{\partial y}\right)_{\text{at } y=0} \quad (15)$$

Where τ_w denoting the local wall shear stress. In terms of transformed variables, these quantities can be written as

$$\frac{1}{2} C_f (\text{Re}_x)^{\frac{1}{n+1}} = -f''(0) \quad (16)$$

The local Nusselt number $N_{u_x} = \frac{q_w x}{k^*(T_f - T_\infty)}$ with q_w as the surface heat flux may be found in terms of the dimensionless temperature at the stretched surface.

$$N_{u_x} = N_u (R_{e_x})^{-\frac{1}{2}} = -\theta'(0) \quad (17)$$

And similarly the surface mass flux found as

$$S_{h_x} = S_h (R_{e_x})^{-\frac{1}{2}} = -\phi'(0) \quad (18)$$

NUMERICAL PROCEDURE

The system of non dimensional, nonlinear, coupled ordinary differential equations (11) to (13) with boundary condition (14) are solved numerically using standard initially value solver the shooting method. For the purpose of this method, the Nactsheim-Swigert shooting iteration technique together with Runge-Kutta six order iteration scheme is taken and determines the temperature and concentration as a function of the coordinate η . In shooting method, the missing (unspecified) initial condition at the initial point of the interval is assumed and the differential equation is integrated numerically as an initial value problem to the terminal point. The accuracy of the assumed missing initial condition is then checked by comparing the calculated value of the dependent variable at the terminal point with its given value there. Selecting a large value may result in divergence of the trial integration or in slow convergence of surface boundary conditions required satisfying the asymptotic outer boundary condition. Selecting too large a value of the independent variable is expensive in terms of computer time. Nachtsheim & Swigert (1965) developed an iteration method, which overcomes these difficulties. Extension of the iteration shell to above equation system of differential equation (14) is straightforward, there are three asymptotic boundary condition and hence three unknown surface conditions $f''(0)$, $\theta'(0)$ and $\phi'(0)$.

RESULTS AND DISCUSSION

To observe the physical significance of the model, the effect of thermal radiation, heat generation and chemical reaction on the MHD power-law fluid flow and heat and mass transfer over a vertical stretching sheet is investigated numerically. In order to get a clear insight of the physical problem, numerical results are displayed with the help of graphical and tabulated illustrations. The numerical values of velocity (f'), temperature (θ) and concentration (ϕ) with the boundary layer have been computed for different parameters as magnetic parameter (M), power-law index (n), thermal conductive parameter (λ), mass convective parameter (λ_M), radiation parameter (N_r), modified Prandtl number (P_r), heat source parameter (Q), chemical reaction parameter (γ) and schmidt number (S_c).

It is possible to compare the results obtained by this numerical method with the previously published work of Azeem & Ramzan (2012). Table 1 and Table 2 shows excellent agreement between the results exists. This lends confidence in the numerical results to be reported subsequently. The comparison Table 1 and Table 2 depicts the numerical results for the local skin friction coefficient and the local Nusselt number for a wide range of values of modified Prandtl, convection parameter, magnetic parameter, and power index. As the physical parameters λ & P_r leads to increases in the local skin friction coefficient at the sheet, this physically means that surface exerts a drag force on the fluid. As increase in P_r decrease the local Nusselt number. The presence of magnetic parameter however makes a significant difference in skin friction coefficient between shear thinning and shear thickening fluids. The physical representation of the present study is shown in Figures 2-15.

Figure 2 displays the dimensionless velocity distribution $f'(\eta)$ for different values of M where $n = 2.0, \lambda = 4.0, \lambda_M = 2.0, Q = 1.0, N_r = 1.0, P_r = 0.71, S_c = 0.6$ and $\gamma = 0.5$. Then for above case it is observed that velocity profiles are decreases as the M increase.

Figure 3 exhibits the dimensionless velocity distribution $f'(\eta)$ for different values of λ where $n = 2.0, M = 2.0, \lambda_M = 2.0, Q = 1.0, N_r = 1.0, P_r = 0.71, S_c = 0.6$ and $\gamma = 0.5$. Then for above case it is

observed that velocity profiles are increases as the λ increase. Here an increase in mixed convection parameter causes a decrease in the inertial force, so resist to the flow will be negligible, hence velocity of the fluid increase.

Figure 4 represent the dimensionless velocity distribution $f'(\eta)$ for different values of λ_M where $n = 2.0, M = 2.0, \lambda = 4.0, Q = 1.0, N_r = 1.0, P_r = 0.71, S_c = 0.6$ and $\gamma = 0.5$. Then for above case it is observed that velocity profiles are decreases as the λ_M increase.

Figure 5 depicts the dimensionless velocity distribution $f'(\eta)$ for different values of P_r where $n = 2.0, \lambda = 4.0, \lambda_M = 2.0, Q = 1.0, N_r = 1.0, M = 2.0, S_c = 0.6$ and $\gamma = 0.5$. Then for above case it is observed that velocity profiles are decreases as the P_r increase.

Figure 6 shows the dimensionless velocity distribution $f'(\eta)$ for different values of N_r where $n = 2.0, \lambda = 4.0, \lambda_M = 2.0, Q = 1.0, P_r = 0.71, M = 2.0, S_c = 0.6$ and $\gamma = 0.5$. Then for above case it is observed that velocity profiles are decreases as the N_r increase.

Figure 7 portrays the dimensionless temperature distribution $\theta(\eta)$ for different values of λ where $n = 2.0, M = 2.0, \lambda_M = 2.0, Q = 1.0, N_r = 1.0, P_r = 0.71, S_c = 0.6$ and $\gamma = 0.5$. Then for above case it is observed that temperature profiles are decreases as the λ increase.

Figure 8 illustrates the dimensionless temperature distribution $\theta(\eta)$ for different values of P_r where $n = 2.0, \lambda = 4.0, \lambda_M = 2.0, Q = 1.0, N_r = 1.0, M = 2.0, S_c = 0.6$ and $\gamma = 0.5$. Then for above case it is observed that temperature profiles are decreases as the P_r increase. Prandtl number controls the relative boundary layer thickness, with an increase in Prandtl number causes to decrease in the thermal diffusivity hence the temperature profiles decreases.

Figure 9 displays the dimensionless temperature distribution $\theta(\eta)$ for different values of Q where $n = 2.0, \lambda = 4.0, \lambda_M = 2.0, P_r = 0.71, N_r = 1.0, M = 2.0, S_c = 0.6$ and $\gamma = 0.5$. Then for above case it is observed that temperature profiles are decreases as the Q increase.

Figure 10 exhibits the dimensionless temperature distribution $\theta(\eta)$ for different values of N_r where $n = 2.0, \lambda = 4.0, \lambda_M = 2.0, Q = 1.0, P_r = 0.71, M = 2.0, S_c = 0.6$ and $\gamma = 0.5$. Then for above case it is observed that temperature profiles are increases as the N_r increase.

Figure 11 represent the dimensionless concentration distribution $\phi(\eta)$ for different values of γ where $n = 2.0, \lambda = 4.0, \lambda_M = 2.0, Q = 1.0, P_r = 0.71, M = 2.0, S_c = 0.6$ and $N_r = 1.0$. Then for above case it is observed that concentration profiles are decreases as the γ increase.

Figure 12 depicts the dimensionless concentration distribution $\phi(\eta)$ for different values of λ_M where $n = 2.0, M = 2.0, \lambda = 4.0, Q = 1.0, N_r = 1.0, P_r = 0.71, S_c = 0.6$ and $\gamma = 0.5$. Then for above case it is observed that concentration profiles are decreases as the λ_M increase.

Figure 13 shows the dimensionless concentration distribution $\phi(\eta)$ for different values of P_r where $n = 2.0, \lambda = 4.0, \lambda_M = 2.0, Q = 1.0, N_r = 1.0, M = 2.0, S_c = 0.6$ and $\gamma = 0.5$. Then for above case it is observed that concentration profiles are increases as the P_r increase.

Figure 14 portrays the dimensionless concentration distribution $\phi(\eta)$ for different values of Q where $n = 2.0, \lambda = 4.0, \lambda_M = 2.0, P_r = 0.71, N_r = 1.0, M = 2.0, S_c = 0.6$ and $\gamma = 0.5$. Then for above case it is observed that concentration profiles are decreases as the Q increase.

Figure 15 displays the dimensionless concentration distribution $\varphi(\eta)$ for different values of N_r , where $n = 2.0, \lambda = 4.0, \lambda_M = 2.0, Q = 1.0, P_r = 0.71, M = 2.0, S_c = 0.6$ and $\gamma = 0.5$. Then for above case it is observed that concentration profiles are increases as the N_r increase.

Table 1. Comparison of the skin friction coefficient $-f''(0)$ for several sets of the different physical parameters when $\lambda_M = Q = S_c = \gamma = 0.0$.

λ	P_r	M	N_r	Azeem and Ramzan (2012)		Present Results	
				$n=1$	$n=2$	$n=1$	$n=2$
0.0	1	1	0.5	1.413680	1.39698	1.414390	1.39702
0.5	1	1	0.5	1.173950	1.10398	1.175229	1.10438
1.0	1	1	0.5	1.950732	0.83773	1.951224	0.83774
1.5	1	1	0.5	0.739883	0.595473	0.746732	0.595476
1	0.5	1	0.5	0.902898	0.772635	0.903129	0.773821
1	0.8	1	0.5	0.932932	0.813171	0.932940	0.813180
1	1.0	1	0.5	0.950732	0.83773	0.950811	0.839823
1	1.5	1	0.5	0.988938	0.891429	0.989243	0.892289
1	1	0.0	0.5	0.488938	0.388492	0.489946	0.389432
1	1	0.5	0.5	0.736441	0.602338	0.736501	0.602467
1	1	1.0	0.5	0.950732	0.837730	0.967450	0.838890
1	1	1.5	0.5	1.14063	1.056730	1.145197	1.056745

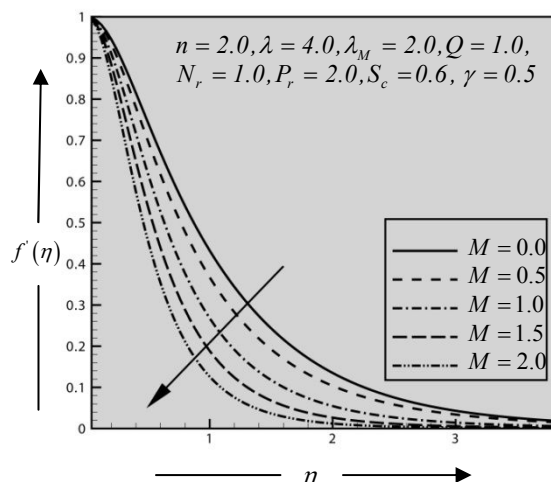


Figure 2. Velocity profiles for different values of Magnetic parameter (M).

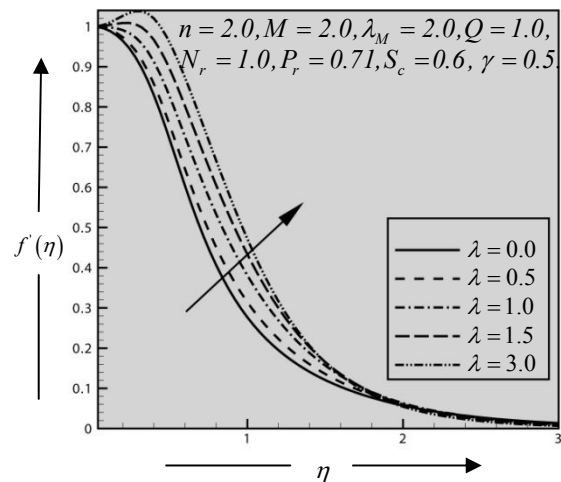


Figure 3. Velocity profiles for different values of thermal conductive parameter (λ).

Table 2. Comparison of the local Nusselt number $-\theta'(0)$ for several sets of the different physical parameters when $\lambda_M = Q = S_c = \gamma = 0.0$.

λ	P_r	M	N_r	Azeem and Ramzan (2012)		Present Results	
				$n=1$	$n=2$	$n=1$	$n=2$
0.0	1	1	0.5	0.676296	0.721520	0.677643	0.721864
0.5	1	1	0.5	0.718889	0.756014	0.718986	0.756321
1.0	1	1	0.5	0.754697	0.787517	0.754785	0.787974
1.5	1	1	0.5	0.985379	0.816495	0.985753	0.817764
1	0.5	1	0.5	0.539607	0.554411	0.539972	0.559732
1	0.8	1	0.5	0.672488	0.697989	0.676532	0.698886
1	1.0	1	0.5	0.754697	0.787517	0.754699	0.789622
1	1.5	1	0.5	0.942255	0.993021	0.942297	0.993124
1	1	0.0	0.5	0.824089	0.848243	0.824167	0.849965
1	1	0.5	0.5	0.786163	0.814362	0.786334	0.815652
1	1	1.0	0.5	0.754697	0.787517	0.754964	0.788842
1	1	1.5	0.5	0.788218	0.765495	0.788219	0.769621

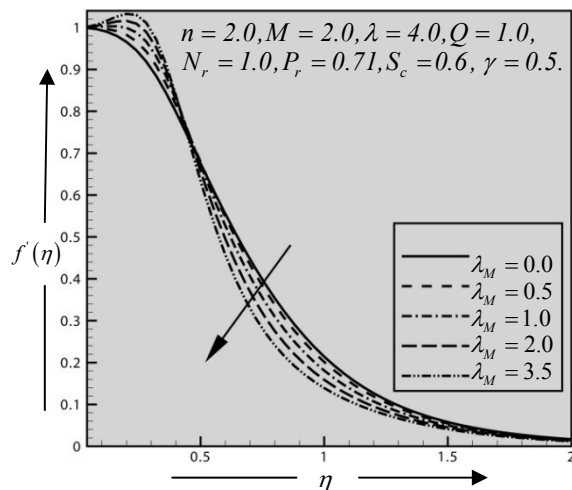


Figure 4. Velocity profiles for different values of mass convective parameter (λ_M).

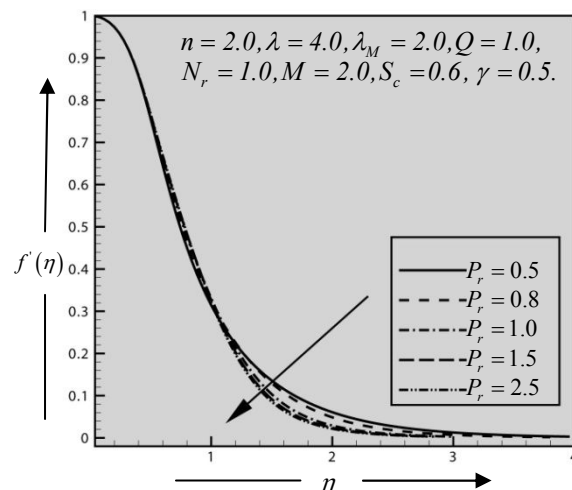


Figure 5. Velocity profiles for different values modified Prandtl number (P_r).

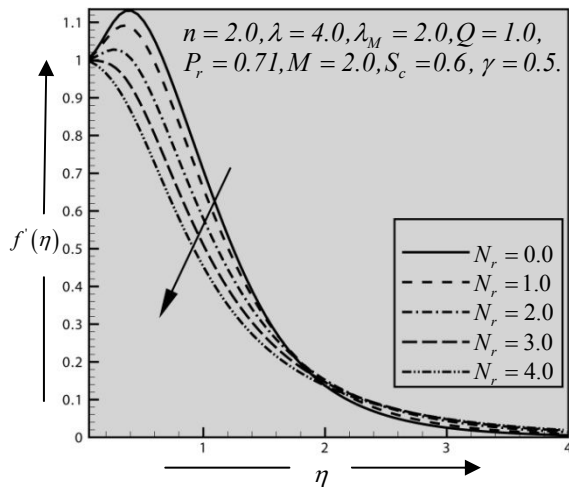


Figure 6. Velocity profiles for different values of Radiation parameter (N_r).

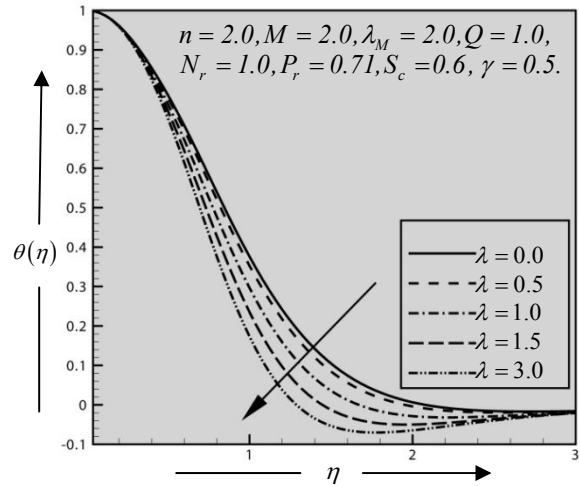


Figure 7. Temperature profiles for different values of thermal conductive parameter (λ).

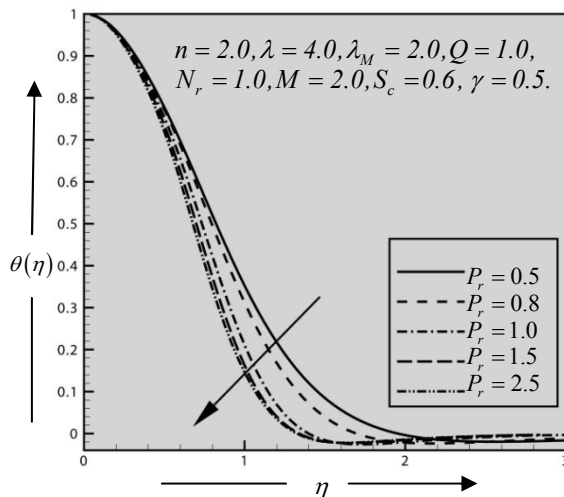


Figure 8. Temperature profiles for different values of modified Prandtl number (P_r).

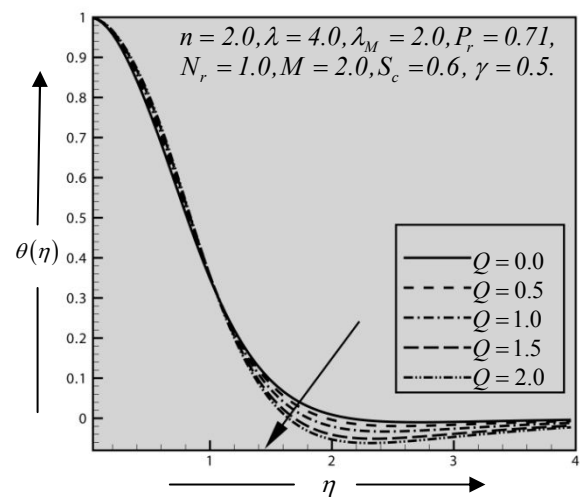


Figure 9. Temperature profiles for different values of heat source parameter (Q).

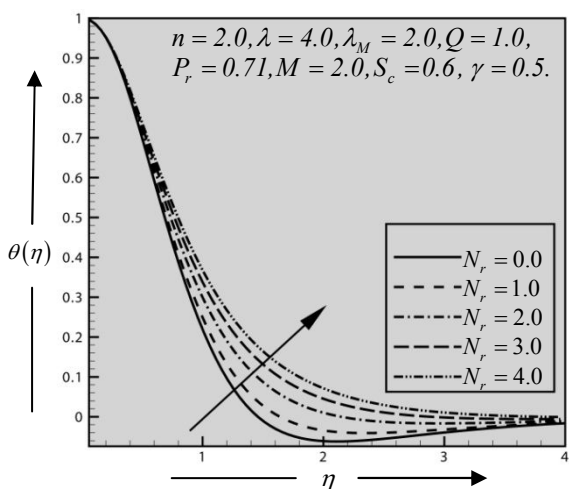


Figure 10. Temperature profiles for different values of Radiation parameter (N_r).

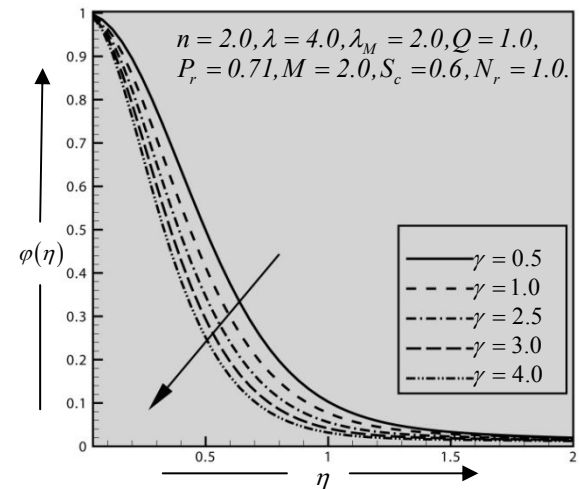


Figure 11. Concentration profiles for different values of chemical reaction parameter (γ).

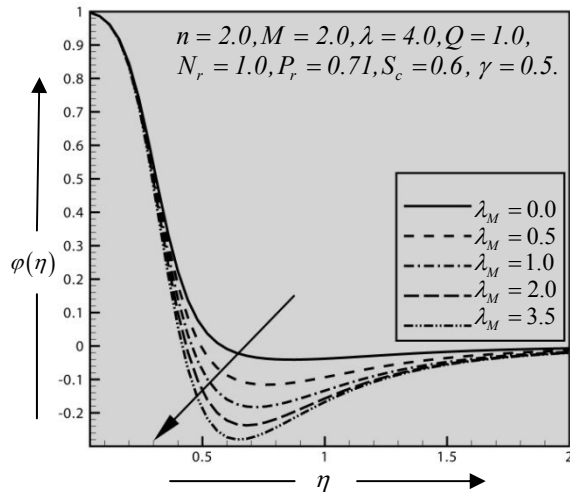


Figure 12. Concentration profiles for different values of mass convective parameter (λ_M).

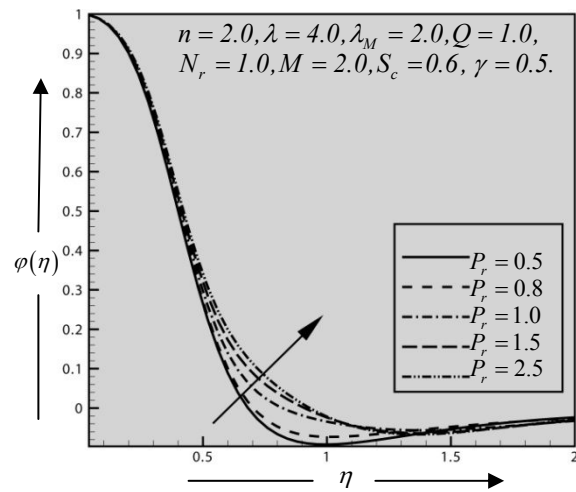


Figure 13. Concentration profiles for different values of modified Prandtl number (P_r).

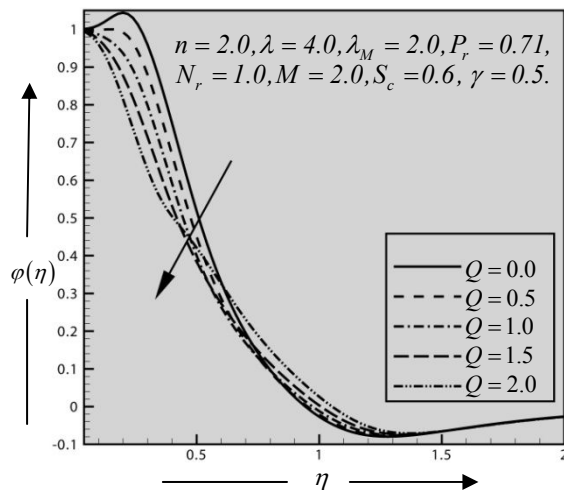


Figure 14. Concentration profiles for different values of heat source parameter (Q).

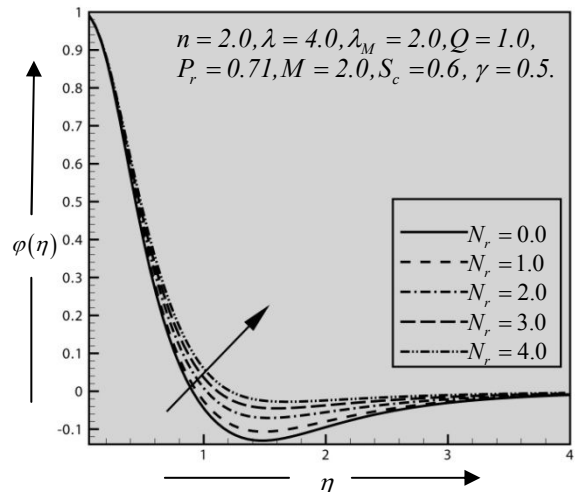


Figure 15. Concentration profiles for different values of Radiation parameter (N_r).

CONCLUSIONS

The present work investigates the problem of Magneto-hydrodynamics mixed convective flow and heat and mass transfer of an electrically conducting non-Newtonian power-law fluid past a vertical stretching surface in the presence of thermal radiation, heat generation and chemical reaction. The governing partial differential equations are transformed into ordinary differential equations by using an appropriate similarity transformation and the resulting boundary value problem is solved numerically by a Nactsheim-Swigert shooting technique together with Runge-Kutta six order iteration schemes. Numerical calculations are carried out for various values of the dimensionless parameters such as the magnetic parameter, power-law index, thermal conductive parameter, mass convective parameter, radiation parameter, modified Prandtl number, heat source parameter and chemical reaction parameter. In order to assess the accuracy of the numerical results the present results are compared with the solution of Azeem & Ramzan (2012) and the comparison shows a good agreement. The following conclusions are drawn from the computed numerical values:

1. Momentum boundary layer thickness decreases as M , P_r , N_r and λ_M increase respectively. Whereas it increases as λ increase.

2. Thermal boundary layer thickness decreases as λ , P_r and Q increase respectively. Whereas it increases as the N_r increase.
3. Concentration boundary layer thickness decreases as γ , λ_M and Q increase respectively. Whereas it increases as P_r and N_r increase respectively.

NOMENCLATURE

a	linear stretching constants
A_1, A_2	constants depends on the fluid properties
B_0	magnetic induction
C_w	concentration at stretching surface
C_∞	ambient concentration as $y \rightarrow \infty$
C_f	skin-friction coefficient
g	acceleration due to gravity
Gr_x	Local Grashof number
Gm_x	Modified Grashof number
k	thermal conductivity
K_r	rate of chemical reaction
M	magnetic parameter
n	Power law index
N_{u_x}	Nusselt number
P	fluid pressure
P_r	Modified prandtl number
Q	heat source parameter
Q_0	heat generation constant
Re_x	local Reynolds number
S_{h_x}	Sherwood number
T_w	temperature at the stretching surface
T_∞	ambient temperature as $y \rightarrow \infty$
u, v	velocity components along x and y axes respectively

Greek symbols

ν	kinematic viscosity
ρc_p	effective heat capacity
α	thermal diffusivity
β	co-efficient of thermal expansion
β^*	co-efficient of mass expansion
γ	chemical reaction parameter
λ	thermal convective parameter
λ_M	mass convective parameter
η	similarity variable
ψ	stream function
$f'(\eta)$	dimensionless velocity
$\theta(\eta)$	dimensionless temperature
$\varphi(\eta)$	dimensionless concentration

Superscript

'	differentiation with respect to η
---	--

Subscripts

w	surface condition
∞	condition far away the surface

REFERENCES

- Acrivos, A. (1960). *A theoretical analysis of laminar natural convection heat transfer to non-Newtonian fluids*, A. I. Ch. E. J. v.6, p.584 -590.
- Andersson, H.I. *et al.*, (1992). *Magnetohydrodynamic Flow of a Power-Law Fluid over a Stretching Sheet*, International Journal of Non-Linear Mechanics, v.27, p.929-936.
- Azeem, S. and Ramzan, A. (2012). *Approximate Analytic Solution for Magneto-Hydrodynamic flow of a Non-Newtonian Fluid over a Vertical Stretching Sheet*, Canadian Journal of Applied Sciences, v.2, p.202-215.
- Brewster, M.Q. (1992). *Thermal Radiative Transfer and Properties*, John Wiley and Sons Inc: New York, USA.
- Char, M.I. (1994). *Heat and Mass Transfer in a Hydromagnetic Flow of a Visco-Elastic Fluid over a Stretching Sheet*, Journal of Mathematical Analysis and Applications, v.186, p.674-689.
- Cheng, P. and Minkowycz, W.J. (1977). *Free convection about a vertical flat plate embedded in a saturated porous medium with applications to heat transfer from a dike*, Journal of Geophysics and Research, v.82, p.2040-2044.
- Cortell, R. (2005). *A Note on Magneto Hydrodynamic Flow of a Power-Law Fluid over a Stretching Sheet*, Applied Mathematics and Computation, v.168, p.557- 566.
- Crane, L.J. (1970). *Flow past a Stretching Plate*, Zeitschrift für Angewandte Mathematik und Physik, v.21, p.645-647.
- Gorla, R.S.R. and Tornabene, R. (1988). *Free convection from a Vertical plate with Non uniform Surface Heat flux and Embedded in a Porous Medium*, Transport in Porous Media Journal, v.3, p.95-106.
- Gorla, R.S.R. and Zinolabedini, A. (1987). *Free convection from a Vertical plate with Non uniform Surface Temperature and Embedded in a Porous Medium*, Transactions of ASME, Journal of Energy Resources Technology, v.109, p.26-30.
- Gupta, P.S. and Gupta, A.S. (1977). *Heat and Mass Transfer on a Stretching Sheet with Suction or Blowing*, The Canadian Journal of Chemical Engineering, v.55, p.744-746.
- Jadhav, J.P. and Waghmode, B.B. (1990). *Heat Transfer to Non-Newtonian Power-Law Fluid past a Continuously Moving Porous Flat Plate with Heat Flux*, Heat and Mass Transfer, v.25, p.377-380.
- Kerehalli, V.P. *et al.*, (2012). *Non-Newtonian Power-Law Fluid Flow and Heat Transfer over a Non-Linearly Stretching Surface*, Applied Mathematics, v.3, p.425-435.
- Khan, M. *et al.*, (2011). *Steady and heat transfer of a magnetohydrodynamic Sisko fluid through porous medium in annular pipe*, International Journal of Numerical and Mathematical Fluids, doi: 10. 1002/flid.2673.
- Lio, S.J. (2005). *A new branch of solutions of boundary layer flows over an incompressible stretching plate*, International Journal of Heat Mass Transfer, v.48, p.2529 – 2539.
- Nachtsheim, P.R. and Swigert, P. (1965). *Satisfaction of the asymptotic boundary conditions in numerical solution of the system of non-linear equations of boundary layer type*, NASA, TND-3004.
- Pavlov, K.B. (1974). *Magnetohydrodynamic Flow of an In-compressible Viscous Fluid Caused by Deformation of a Plane Surface*, Magninaya Gidrodinamika (USSR), v.4, p.146-147.
- Sarpakaya, T. (1961). *Flow on Non-Newtonian Fluids in a Magnetic Field*, AIChE Journal, v.7, p. 26-28.
- Schawalter, W.R. (1960). *The application of boundary layer theory to power law pseudo plastic: sunukar solutions*, A. I. Ch. E. J., v.6, p.24- 28.
- Zhongzin, Z. and Junyu, W. (2007). *On the similarity solution of magnetohydrodynamic flows of power-law fluids over a stretching sheet*, Journal of Math. Anal. Appl., v.330, p.207 – 220.